MNRAS: in press

# Precessing collimated outflows in the planetary nebula IC 4846

Luis F. Miranda

*Instituto de Astrofísica de Andalucía, CSIC, Apdo. Correos 3004, E-18080 Granada, Spain*

lfm@iaa.es

Martín A. Guerrero

*Department of Astronomy, University of Illinois at Urbana-Champaign 1002 West Green Street, Urbana, IL 61801 USA*

mar@astro.uiuc.edu

José M. Torrelles

*Institut d'Estudis Espacials de Catalunya (IEEC/CSIC) and Instituto de Ciencias del Espacio (CSIC), Edifici Nexus, C/ Gran Capitá 2-4, E-08034 Barcelona, Spain*

torrelles@ieec.fcr.es

## ABSTRACT

We present [N II] and H$\alpha$ images and high resolution long–slit spectra of the planetary nebula IC 4846, which reveal, for the first time, its complex structure and the existence of collimated outflows. The object consists of a moderately elongated shell, two (and probably three) pairs of collimated bipolar outflows at different orientations, and an attached circular shell. One of the collimated pairs is constituted by two curved, extended filaments whose properties indicate a high velocity, bipolar precessing jet. A difference of $\simeq 10$ km s$^{-1}$ is found between the systemic velocity of the precessing jets and the centroid velocity of the nebula, as recently report for Hu 2-1. We propose that this difference is due to orbital motion of the ejection source in a binary central star. The orbital separation of $\leq 30$ AU and period $\leq 100$ yr estimated for the binary are similar to those in Hu 2-1, linking the central stars of both planetary nebulae to interacting binaries. Extraordinary similarities also exist between IC 4846 and the bewildering planetary nebula NGC 6543, suggesting a similar formation history for both objects.

*Subject headings:* planetary nebulae: individual: (IC 4846) – ISM: kinematics and dynamics – ISM: jets and outflows

## 1. Introduction

IC 4846 (PN G 027.6−09.6) is a compact planetary nebula (PN) whose morphology has not been studied in detail yet. The only available information on its structure is provided by the VLA 6 cm continuum observations by Kwok (1985, see also Aaquist & Kwok 1990), showing several knots embedded in a faint elongated structure of $\simeq 3\times2$ arcsec$^2$ in size. The H$\beta$ surface brightness ($\log F(\mathrm{H}\beta) = -11.34$, Acker et al. 1992) suggests that IC 4846 has a high electron density. This is corroborated by the small [S II]$\lambda$6717,$\lambda$6731 doublet ratio (Barker 1978; Acker et al. 1992) which reaches the limiting ratio for high electron density ($N_\mathrm{e} \gtrsim 10^4$ cm$^{-3}$). Both its small angular size and high density indicate that IC 4846 is a young PN. The line intensity ratios (Acker et al. 1992) point to a moderate excitation ([N II]$\lambda$6583/H$\alpha \simeq 0.07$, [O III]$\lambda$4959/H$\beta \simeq 3.7$, and very faint He II $\lambda$4686). *IUE* low-resolution UV spectra of the central star show a strong P-Cygni profile in the N V line[1] with a terminal velocity of $\simeq 1300$ km s$^{-1}$. The occurrence of a strong stellar wind in the central stars of PNe is indicative of their early evolutionary stage (Cerruti-Sola & Perinotto 1985).

The shaping processes of PNe occur early in their formation. Therefore, the signatures of these processes in the nebula are more recent and more likely to have withstood the fast nebular evolution in young PNe. This turns the observations of young PNe of chief importance in the understanding of their formation mechanisms. Accordingly, IC 4846 was included in our observational program of compact young PNe (see Miranda 1999 and references therein), and narrow–band H$\alpha$ and [N II] images and long–slit high–resolution spectra were obtained to study its structure and internal kinematics. The results reported in this paper evidence the existence of bipolar, precessing collimated outflows in IC 4846.

## 2. Observations

Direct images of IC 4846 were obtained in 1997 July 24 with the Nordic Optical Telescope (NOT) at Roque de los Muchachos Observatory on La Palma[2]. The detector was a LORAL 15 $\mu$m CCD at the HIRAC camera providing a plate scale of 0.11 arcsec pixel$^{-1}$. The filters were H$\alpha$ ($\lambda_0 \simeq 6563$ Å, FWHM $\simeq 10$ Å), and [N II] ($\lambda_0 \simeq 6584$ Å, FWHM $\simeq 10$ Å). Exposure times were 900 s in each case. The spatial resolution is $\simeq 1$ arcsec. The images were bias subtracted and flat–fielded following standard procedures within MIDAS package.

Long–slit echelle spectra of IC 4846 were taken with the IACUB[3] spectrograph at the NOT in

[1]Based on INES data from the *IUE* satellite.

[2]The Nordic Optical Telescope is operated on the Island of La Palma by NOTSA in the Spanish Observatorio del Roque de los Muchachos of the Instituto de Astrofísica de Canarias

[3]The IACUB uncrossed echelle spectrograph was built in a collaboration between the IAC and the Queen's University of Belfast

1998 August 2. The detector was a Thompson 19 $\mu$m CCD with 1024×1024 pixels. A filter was used to isolate the H$\alpha$ and [N II]$\lambda$6583 emission lines in the $9^{th}$ echelle order. A Thorium–Argon spectrum was taken after each object spectrum for wavelength calibration purposes. Exposure time was 1800 s for each spectrum. The observed position angles (PAs) were 11°, 30°, 54°, and 140° with the slit centered on the object. The dispersion was 2.5 Å $mm^{-1}$, and the achieved spectral resolution (FWHM) $\simeq$ 7.5 km $s^{-1}$. The spatial resolution is $\simeq$ 1.5 arcsec. Absolute errors in the radial velocity are $\pm$ 1.5 km $s^{-1}$, whereas relative errors (within each long-slit spectrum) are $\pm$ 0.5 km $s^{-1}$. The data were reduced following standard procedures for long–slit spectroscopy within the IRAF and MIDAS packages. Thereafter the [N II]$\lambda$6583 emission line will be referred to as the [N II] line.

## 3. Results

### 3.1. General structures

Figures 1 and 2 present grey–scale and contour maps, respectively, of IC 4846 in the light of [N II] and H$\alpha$. The morphology of IC 4846, resolved in these images for the first time, displays a great wealth of structures. At the lowest intensity levels, the appearance of the nebula is elliptical with two bipolar features protruding at PA $\simeq$ 54°. These features, denoted A1–A2 (Fig. 2), are curved filaments enhanced in [N II]. A second, inner ellipse, observed in H$\alpha$ and [N II] at intermediate intensity levels, can be recognized with its major axis at PA $\simeq$ 11°. Two compact knots, B1–B2, are observed at the tips of this inner ellipse. The innermost regions of IC 4846 are dominated in [N II] at the highest intensity levels by two bright structures, C1–C2, which are not clearly distinguished in the H$\alpha$ image. An additional attached circular shell with a size of $\simeq 10''$ can also be identified in the H$\alpha$ image.

In order to emphasize the different structures of IC 4846 described before, we have obtained deconvolved images using the Lucy-Richardson algorithm as implemented in the MIDAS package. Deconvolved H$\alpha$ and [N II] images to a resolution of $\simeq$ 0.5 arcsec (obtained with 30 iterations) are also presented in Fig. 2. These images clearly show the structural richness of the nebula. In particular, the curvature and filamentary appearance of A1–A2 can easily be recognized as well as the compactness of B1–B2. C1–C2 appear as point–symmetric structures elongated perpendicular to the radial direction from the center. In H$\alpha$ the inner regions appear as an arc with an asymmetric intensity distribution. We note that the inner regions of the nebula resemble the morphology observed at 6 cm (Kwok 1985). In addition, the inner shell presents a very low ellipticity.

Figure 3 shows position–velocity (PV) contour maps of the high resolution long–slit spectra of the [N II] emission line at PAs 11°, 54° and 140°. The spectrum at PA 30° is similar to that at PA 11° and is not shown here. The bipolar features A1–A2, B1–B2 and C1–C2 can be identified in the PV maps with point-symmetric pairs of components. We also note that no *closed* velocity ellipse can be identified in the PV maps of the [N II] emission line, which could be expected from

the elliptical structures observed in the images. The H$\alpha$ spectra (not shown here) are dominated by emission from the inner regions. These regions show a tilt in the PV maps similar to the tilt of C1–C2 (Fig.3). A1–A2 are clearly distinguished because of their high radial velocity. B1–B2 seem to be present, too, although the H$\alpha$ line is not useful for a detailed kinematic study owing its large thermal width.

A [N II]/H$\alpha$ ratio map is also presented in Fig 1. A1–A2 and B1–B2 are highlighted due to their relatively strong [N II] emission. C1–C2 can also be recognized, although the line ratio seems to have lower values. A quantitative estimate of [N II]/H$\alpha$ should be worked out using the long-slit spectra in order to single out both spatially and kinematically the different components. PV maps of the [N II]/H$\alpha$ ratio for PAs 11° and 54° are shown in Fig. 3. A mean value of [N II]/H$\alpha$ in the nebula of $\simeq 0.06$ is obtained, similar to that obtained by Acker et al. (1992). The three pairs present enhanced [N II] emission, with mean [N II]/H$\alpha$ values of $\simeq 0.8$ (A1–A2), $\simeq 0.15$ (B1–B2), and $\simeq 0.2$ (C1–C2), which are a factor 2.5 to 13 higher than the mean ratio in the nebula. Furthermore, peak values of this ratio up to $\simeq 1.5$ are found in A1–A2, and up to $\simeq 0.3$ in B1–B2 and C1–C2. Common to all three pairs is that [N II]/H$\alpha$ peaks at larger distances from the center than the [N II] emission peaks (see also Fig. 1).

Table 1 lists different parameters of the bipolar pairs as deduced from the [N II] images and long–slit spectra. In order to deduce systemic velocities, we have first considered the centroid of each bipolar pair as representative of its own systemic velocity. The systemic velocity obtained for each pair is listed in Table 1. Secondly, we have obtained the centroid velocity of the [N II] emission line as representative of the systemic velocity of the whole nebula. In order to avoid the contribution of the bipolar pairs, the centroid velocity was obtained from the middle point of the spatially integrated emission at 10% level of the intensity peak. We obtain $V_{sys}$(centroid) $\simeq 168$ km s$^{-1}$ and note that an identical value is obtained if the middle point is considered at 5% or 15% levels of the intensity peak. The values for $V_{sys}$(centroid), $V_{sys}$(B1–B2) and $V_{sys}$(C1–C2) agree within the absolute errors with the value quoted by Bianchi (1992) and Durand et al. (1998) for the systemic velocity of IC 4846. The systemic velocity of B1–B2 and C1–C2 are almost identical to each other; both are slightly blueshifted ($\simeq 3.5$ km s$^{-1}$) with respect to the centroid velocity. In the case of A1–A2, its systemic velocity is noticeably blueshifted by $\simeq 10$ km s$^{-1}$ with respect to the centroid velocity. We will discuss in § 4 possible interpretations for these systemic velocity shifts. In the following, radial velocities of each pair will be quoted with respect to its own systemic velocity.

### 3.2. Properties of the collimated components

IC 4846 displays three pairs of structures, A1–A2, B1–B2, and C1–C2, which are highly evocative of collimated outflows. We describe as follows the properties of these components.

A1–A2 appear detached and off-axis ($\Delta$(PA) $\simeq 43°$) with respect to the major axis of the

inner ellipse. Their orientation changes by $\simeq 5°$–$10°$. A1–A2 can be traced along $\simeq 6$ arcsec, which represents a considerable fraction of the total nebular size. An upper limit of $\simeq 1$ arcsec is obtained for their lateral size. The radial velocity systematically varies along A1–A2: a minimum velocity of $\simeq \pm 36$ km s$^{-1}$ is observed at the minimum angular distance; the velocity then steadily increases with the distance up to $\simeq \pm 52$ km s$^{-1}$; finally, it slightly decreases at the tips of the features. The velocity width is small as compared with the velocity difference between A1 and A2 (see Table 1), which implies a high degree of collimation. According to their properties, A1–A2 are highly suggestive of a precessing bipolar jet.

B1–B2 present a rather moderate radial velocity and the velocity width is small and comparable to that of A1–A2 (Table 1). The small velocity width and the compactness indicate that B1–B2 are highly collimated outflows.

The radial velocity of C1–C2 does not depend on the PA (Fig. 3, Table 1), although some small variations ($\simeq 7$ km s$^{-1}$) within C1–C2 are observed. Possible interpretations of this pair will be discussed in § 4.

## 4. Discussion

The observations of IC 4846 have disclosed a complex structure composed of three different elements: (1) two apparent elongated shells with different orientations, (2) an attached circular shell and (3) three pairs of point-symmetric components at different orientations with typical properties of collimated outflows. In the following we discuss about the nature, models and possible interpretations of these components.

As already mentioned, there is no kinematic evidence for the elliptical shells in the PV maps of the [N II] line, although the extended emission observed in the PV maps may be related to these shells. We also note that the major axis of the outer ellipse is only defined by A1–A2. In fact, without A1–A2 the outer ellipse could not be recognized. Images at higher resolution would be necessary to elucidate the precise geometry of these shells. While A1–A2 and B1–B2 can be interpreted as precessing bipolar outflows, the interpretation of the pair C1–C2 is somewhat difficult. Its kinematic properties and the elongation perpendicular to the radial direction suggest that C1–C2 could represent collimated ejections in which the orientation of the ejection axis has remarkably changed over the ejection time. However, we cannot completely rule out that C1–C2 represents a ring-like structure containing two bright opposite regions. The attached circular shell probably represents a previous slow wind ejected by the AGB progenitor of IC 4846. It is similar to other attached shells observed in PNe and its formation may be related to the dynamics of ionization fronts (see Mellema 1995 and references therein).

In the scenario that A1–A2 are precessing bipolar jets, we can obtain estimates for the inclination angle and velocity by assuming that the expansion velocity is constant and that the variation of the radial velocity is due to a systematic change of the angle between the observer and the

precessing jet along a precession cone with aperture angle $\simeq 5°$–$10°$. The observed minimum and maximum radial velocities are assumed to be related to the far and rear side of the precession cone, respectively. Using the model for a biconical flow described by Miranda & Solf (1992), we obtain an inclination angle for the precession axis of $\simeq 13°$–$26°$ with respect to the plane of the sky, and a velocity of $\simeq$ 100–190 km s$^{-1}$. The (mean) kinematic age is $\simeq 200\times$D(kpc) yr, where D is the distance to IC 4846, which is extremely uncertain with published values between 2 and 11 kpc (see Acker et al. 1992). The images also show that A1–A2 protrude from the circular shell. This result, the increase of the [N II]/H$\alpha$ ratio at larger distances and the decrease of the radial velocity at the tips of A1–A2 suggest an interaction between the jet fronts and the circular shell, in a similar way to that reported in, e.g., NGC 6891 (Guerrero et al. 2000).

It is worthwhile to emphasize the extraordinary similarity between IC 4846 and the well-known PN NGC 6543 (see Miranda & Solf 1992 and Reed et al. 1999). The following structural components are common to these two PNe (we will use for NGC 6543 the nomenclature of Miranda & Solf 1992):

1. *Basic elongated shell(s).* In NGC 6543 two shells are observed, an outer bipolar shell with a bright ring between the lobes and an inner elliptical one. In IC 4846 two elongated shells are suggested by the images (but see above). The possible existence of an equatorial ring should be confirmed by new data.

2. *Bipolar knots at the tips of the shell.* The knots FF' in NGC 6543 correspond to B1–B2 in IC 4846.

3. *Precessing bipolar jets.* The bipolar jets JJ' in NGC 6543 correspond to A1–A2 in IC 4846. The similarity between JJ' and A1–A2 is extraordinary. Both appear off-axis with respect to the orientation of the basic shell and are curved, with a change of orientation of $5°$–$10°$. The radial velocity presents an identical variation along the jets with a steady increase up to a maximum radial velocity and a small decrease at their tips. Finally, an expansion velocity of $\simeq$ 100–200 km s$^{-1}$ is obtained in both cases.

4. *Point-symmetric components perpendicular to the radial direction.* C1–C2 in IC 4846 could correspond to DD' in NGC 6543.

There are some differences between both objects, but these are most likely attributable to different orientations, ages and distances. Whatever these differences, the conspicuous kinematic and structural similarities lead us to conclude that NGC 6543 and IC 4846 have shared a similar formation history.

An interesting result in IC 4846 is the systemic velocity shifts among the different components and the centroid of the nebula. In the case of B1–B2 and C1–C2, the shifts are only slightly larger than the relative errors and we cannot conclude whether they are real. In the case of A1–A2, however, the shift is noticeable and we consider it real. Both the remarkable spatial and velocity symmetry observed in A1–A2 exclude that this shift may be ascribed to different ejection velocity,

changes (deceleration) in the velocity in one of the components of the pair, different ejection angle or a combination of the three. A more plausible explanation is that the systemic velocity of A1–A2 is indeed intrinsically different from that of the other components and, in particular, from that of the emission centroid. Similar shifts in the systemic velocity of collimated outflows and shell have been recently reported in the PN Hu 2-1 (Miranda et al. 2000). Furthermore, both PNe share the presence of two systems of collimated outflows at different orientations, one of them projected along the nebular major axis and one off-axis, suggesting a parallel formation history. Moreover, inspection of the kinematic data of NGC 6543 (see Miranda & Solf 1992) suggests that a difference of $\sim 7$ km s$^{-1}$ could exist between the systemic velocity of JJ' and the systemic velocity of the nebula as defined by the rest of components. In the case of Hu 2-1, the shifts of systemic velocity have been interpreted as a direct evidence of orbital motion of the ejection source in a binary central star (Miranda et al. 2000). The velocity shifts detected in IC 4846 fit also into this framework. If A1–A2 are ejected from a star in a binary system, the space velocity of the A1–A2 will contain an additional velocity component due to the orbital motion, besides to the component due to the own ejection velocity. Accordingly, the systemic velocity of A1–A2 will be shifted from that of the emission centroid of the nebula (see Miranda et al. 2000 for details). We note that the same would apply to B1–B2 and C1–C2 if their observed velocity shifts were real.

The systemic velocity shift of A1–A2 (10 km s$^{-1}$) is very similar to that found in Hu 2-1 (8 km s$^{-1}$) and in NGC 6543 (7 km s$^{-1}$). Consequently, the orbital parameters of their binary central stars should be rather similar as well, with an orbital separation $\leq 30$ AU and an orbital period $\leq 100$ yr, thus linking the central stars of these nebulae to symbiotic stars. These results strongly suggest that the central star of IC 4846, similarly to that of Hu 2-1 and NGC 6543, is a binary star in which mass transfer from a red giant leads to the formation of an accretion disk about a secondary (Mastrodemos & Morris 1998, 1999), from which collimated ejections may be generated.

## 5. Conclusions

Narrow–band imaging and high–resolution spectroscopy of the PN IC 4846 in the [N II]$\lambda$6583 and H$\alpha$ lines have revealed a complex structure similar in many respects to that of NGC 6543. The most remarkable components in IC 4846 are three pairs of point-symmetric structures oriented at different directions. Two (and probably the three) pairs represent collimated bipolar outflows. The kinematics and morphology of the pair observed at PA 54° (A1–A2) are highly suggestive of a precessing jet moving at $\simeq$ 100–200 km s$^{-1}$. Furthermore, the velocity shift between their systemic velocity and that of the nebula can be interpreted as a result of orbital motion of the ejection source in a binary central star. This kind of systemic velocity differences has also been observed in Hu 2-1 and could be present in NGC 6543. Thus, the formation of IC 4846 (and Hu 2-1 and NGC 6543) could be related to physical processes in the own evolution of interacting binary stars.

**Acknowledgments**

We thank our referee for his/her valuable comments which have improved the presentation of the paper. LFM and JMT are supported partially by DGESIC PB98-0670-C02 and Junta de Andalucía (Spain). MAG is supported partially by DGESIC of the Spanish Ministerio of Educación y Cultura.

**References**

Aaquist O.B., Kwok S., 1990, A&AS, 84, 229

Acker A., Ochsenbein F., Stenholm B., Tylenda R., Marcout J., Schohn C., 1992, Strasburg-ESO Catalogue of Galactic Planetary Nebulae. ESO, Garching

Barker T., 1978, ApJ, 219, 914

Bianchi L., 1992, A&A, 260, 314

Cerruti–Sola M., Perinotto M., 1985, ApJ, 291, 237

Durand S., Acker A., Zijlstra A., 1998, A&AS, 132, 13

Guerrero M.A., Miranda L.F., Manchado A., Vázquez R., 2000, MNRAS, 313, 1

Kwok S., 1985, AJ, 90, 49

Mastrodemos N., Morris M., 1998, ApJ, 497, 303

Mastrodemos N., Morris M., 1999, ApJ, 523, 357

Mellema G., 1995, MNRAS, 277, 173

Miranda L.F., 1999, in ASP Conf. Ser., vol.188, p. 257

Miranda L.F., Solf J., 1992, A&A, 260, 397

Miranda L.F., Torrelles J.M., Guerrero M.A., Vázquez R., Gómez Y., 2000, MNRAS, in press

Reed D.S., Balick B., Hajian, A.R., Klayton T.L., Giovanardi, S., Casertano S., Panagia N., Terzian Y., 1999, AJ, 118, 2430

**Table 1: Parameters of the [N II] bipolar pairs in IC 4846**[a]

| Pair | $\delta V_r$ [b] ($km\,s^{-1}$) | $\Delta V$ [c] ($km\,s^{-1}$) | $V_{sys}$(LSR) [d] ($km\,s^{-1}$) | $\delta V_{sys}$ [e] ($km\,s^{-1}$) | $\delta X$ [f] (arcsec) | PA [g] (degrees) |
|---|---|---|---|---|---|---|
| A1–A2 | 96 | 20 | 158 | −10 | 7.4 | 54 |
| B1–B2 | 26 | 18 | 164 | −4 | 5.4 | 11 |
| C1–C2 | 38 | 22 | 165 | −3 | 1.8 | 25 |

[a] Obtained from the images and long–slit [N II] spectra shown in Figs. 1 and 3, respectively.
[b] Separation in radial velocity between intensity peaks of the components of each pair.
[c] Velocity dispersion (FWHM) corrected of instrumental resolution.
[d] Systemic velocity.
[e] Maximum difference between $V_{sys}$(LSR) for each pair and $V_{sys}$(LSR) for the centroid of the [N II] emission line = 168 $km\,s^{-1}$
[f] Projected angular separation between the intensity peak of the components of each pair .
[g] Orientation (position angle).

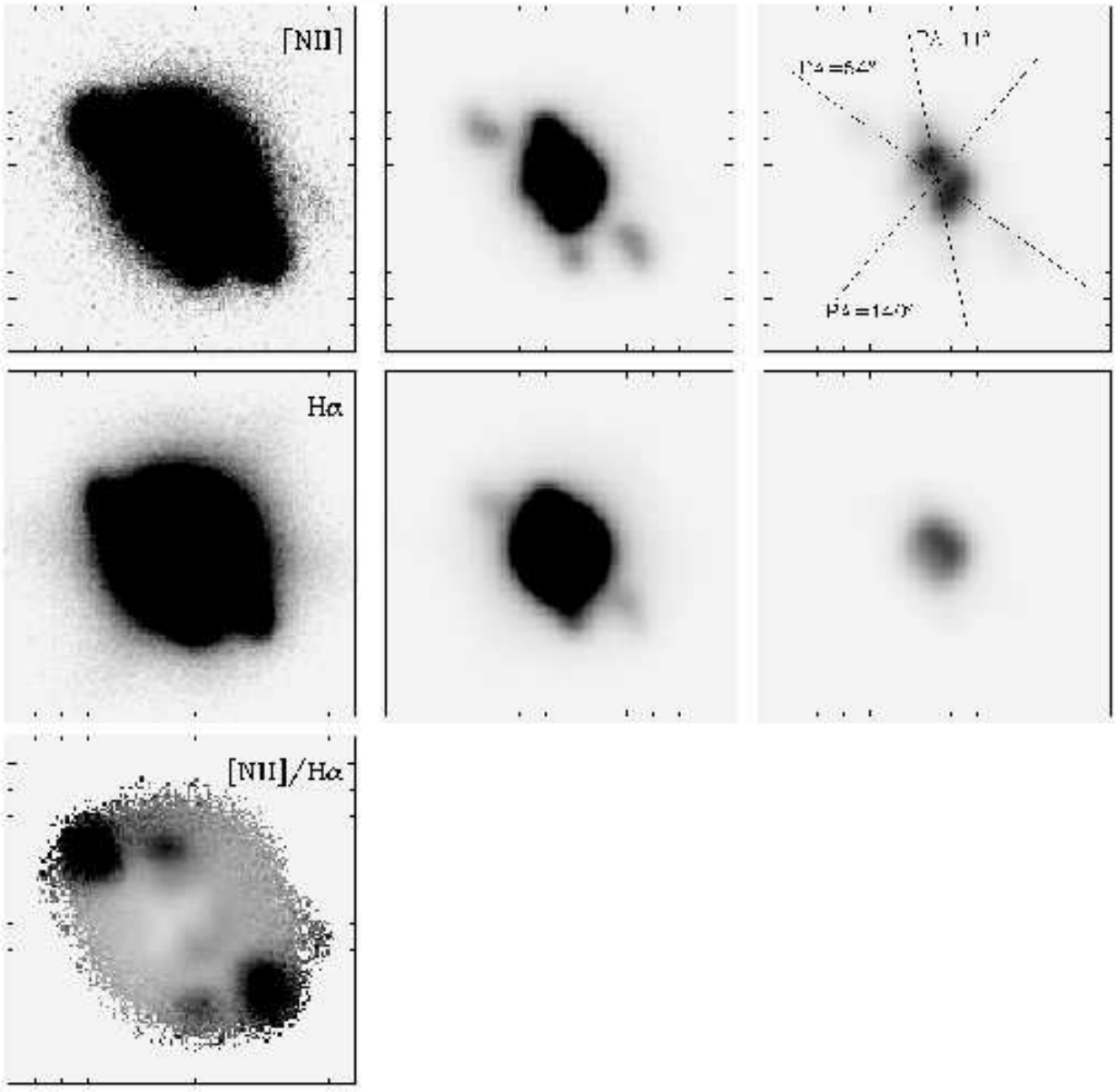


Fig. 1.— Grey–scale maps of the [N II]λ6583 *(upper row)*, Hα *(middle row)* and [N II]λ6583/Hα *(lower row)* images of IC 4846. The [N II] and Hα images are presented in three different contrasts in order to show the faint and bright nebular regions. The observed slit positions at PAs 11°, 54° and 140° are indicated in one of the [N II] maps. In the [N II]/Hα map, black indicates stronger [N II] emission. North is up, east to the left. The size of the field shown is 14×14 arcsec$^2$.

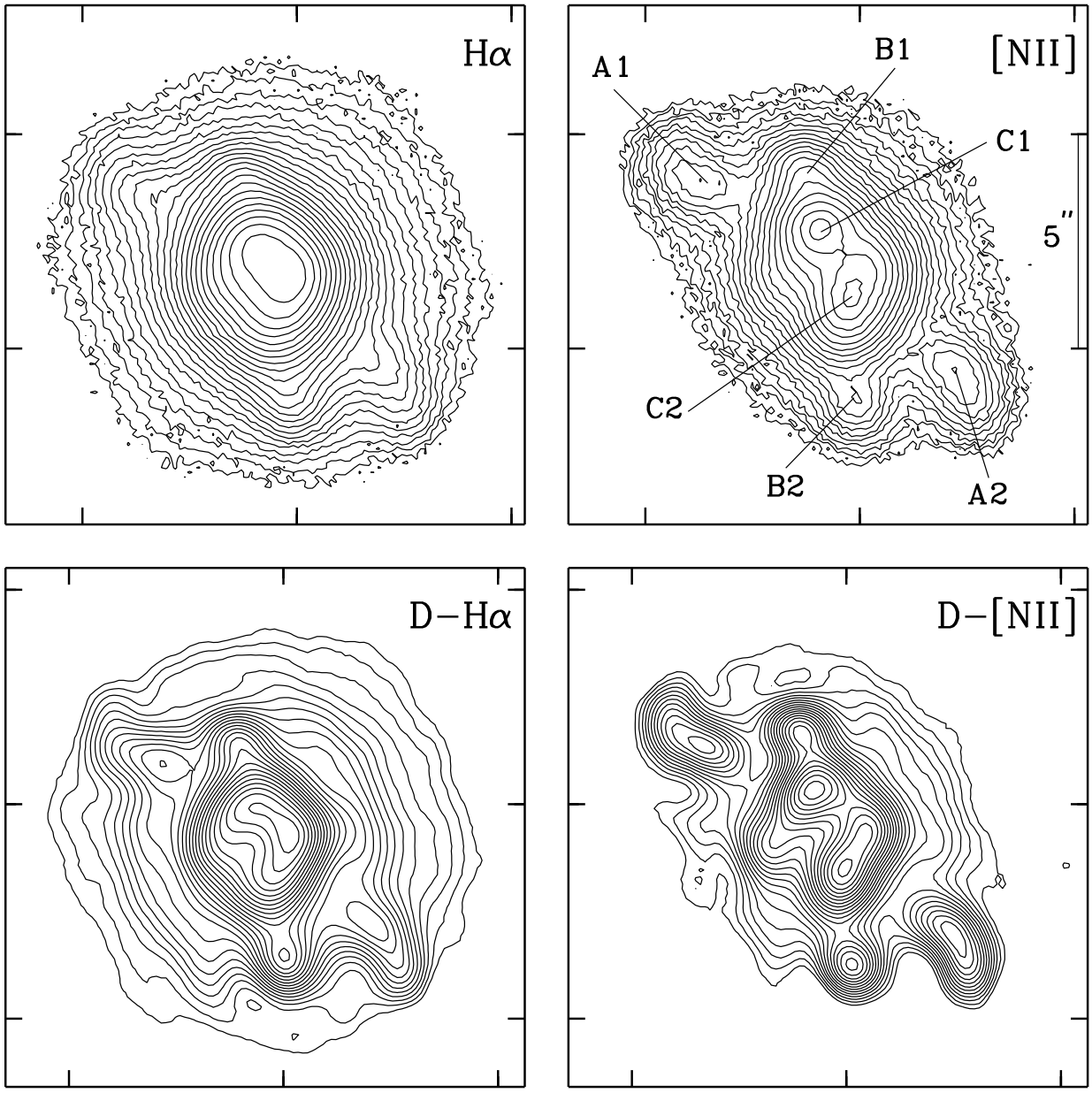


Fig. 2.— *(upper row)* Contour plots of the images of IC 4846 presented in Fig. 1. The pairs of bright [N II] components are labeled A1–A2, B1–B2 and C1–C2. *(lower row)* Deconvolved H$\alpha$ and [N II] images at a resolution of 0.5 arcsec. The contours are logarithmic separated by a factor 1.32 in intensity.

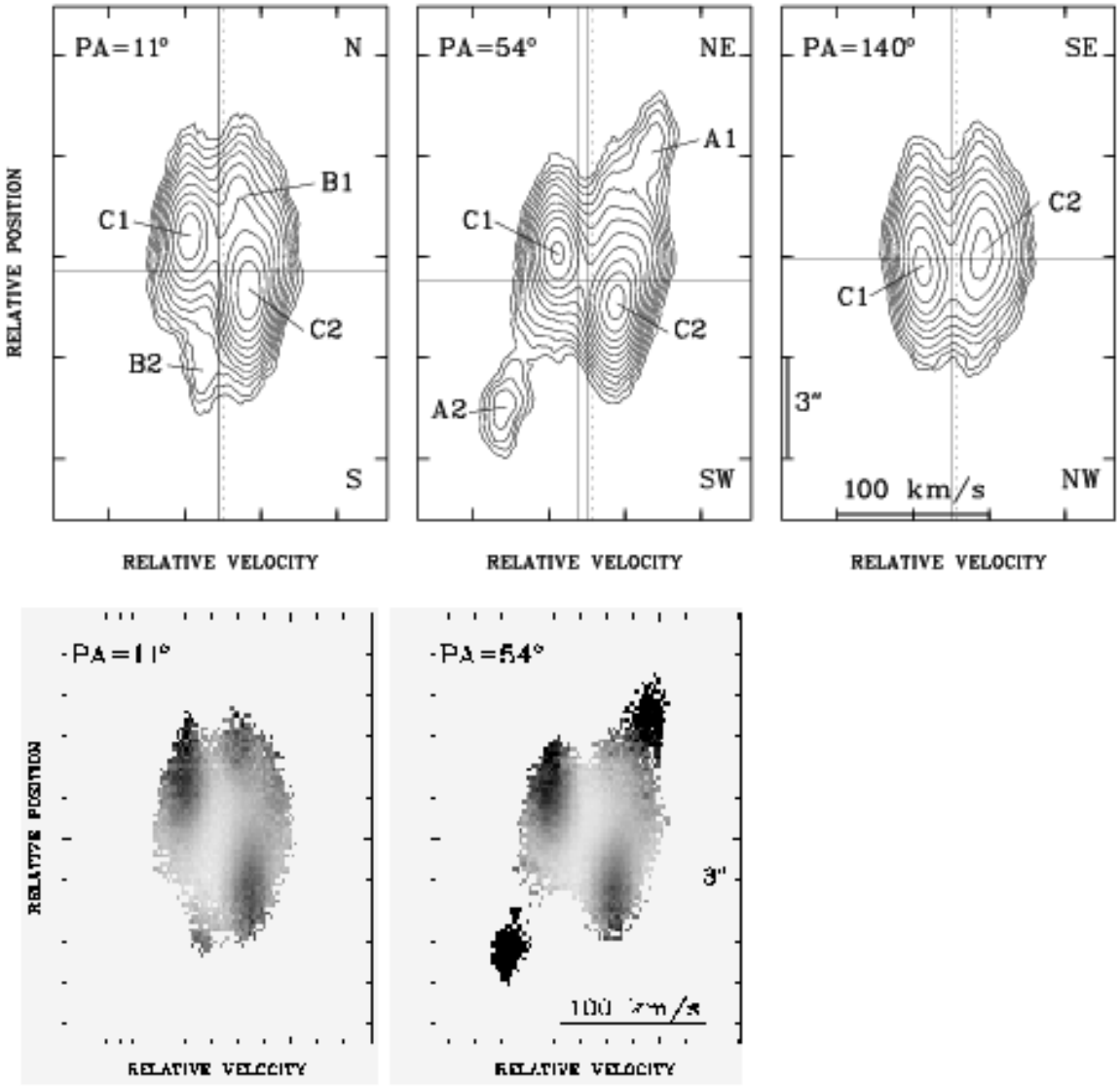


Fig. 3.— *(upper row)* Contour plots of the long–slit [N II]$\lambda$6583 spectra at three different PAs (upper left) in a position–velocity representation. The contours are logarithmic separated by a factor 1.41 in intensity. The identified components are labeled (see Fig. 2). The horizontal line corresponds to the mean position of C1–C2. The vertical lines correspond to the systemic velocity of the different pairs (continuous lines) and to that of the emission centroid (dashed line) (see text). *(lower row)* Grey–scale maps of the [N II]$\lambda$6583/H$\alpha$ ratio deduced from the long–slit spectra of IC 4846 at PAs 11° and 54°. Black indicates stronger [N II] emission.